

# Orthogonally polarized dual-wavelength Nd:YAlO<sub>3</sub> laser at 1341 and 1339 nm and sum-frequency mixing for an emission at 670 nm

Yanfei Lü,<sup>1,\*</sup> Jing Xia,<sup>1</sup> Jing Zhang,<sup>2</sup> Xihong Fu,<sup>3</sup> and Huilong Liu<sup>1</sup>

<sup>1</sup>School of Physical Science and Technology, Yunnan University, Kunming 650091, China

<sup>2</sup>School of Science, Changchun University of Science and Technology, Changchun 130022, China

<sup>3</sup>State Key Laboratory of Luminescence and Applications, Changchun Institute of Optics, Fine Mechanics and Physics, Chinese Academy of Sciences, Changchun 130033, China

\*Corresponding author: [optik@sina.com](mailto:optik@sina.com)

Received 28 April 2014; revised 9 July 2014; accepted 13 July 2014;  
posted 14 July 2014 (Doc. ID 210917); published 6 August 2014

We report a diode-pumped continuous wave (cw) orthogonally polarized dual-wavelength laser at 1339 and 1341 nm with a single *b*-cut Nd:YAlO<sub>3</sub> (Nd:YAP) crystal. By adjusting the tilt angle of the uncoated glass plate inserted in the laser cavity, we can control the cavity losses of two polarized directions. The output wavelengths are 1339 nm in *a*-axis polarization and 1341 nm in *c*-axis polarization, respectively, which are orthogonal to each other. At an incident pump power of 17.3 W, the cw output power obtained at 1339 and 1341 nm is 1.6 and 2.3 W, respectively. Furthermore, intracavity sum-frequency mixing at 1339 and 1341 nm was then realized in a KTiOPO<sub>4</sub> (KTP) crystal to reach the red range. To our knowledge, this is the first work realizing an orthogonally polarized dual-wavelength Nd:YAP laser based on the <sup>4</sup>*F*<sub>3/2</sub>–<sup>4</sup>*I*<sub>13/2</sub> transition. Such a dual-wavelength laser would be especially valuable as a compact laser source to generate terahertz emission because the frequency difference between 1339 and 1341 nm is about 0.9 THz. © 2014 Optical Society of America

OCIS codes: (140.3410) Laser resonators; (140.3580) Lasers, solid-state.

<http://dx.doi.org/10.1364/AO.53.005141>

## 1. Introduction

Orthogonally polarized dual-wavelength lasers are new attractive devices for various applications, such as laser interferometry and precision metrology [1,2], especially for precise measurements of length, displacements, angle, velocity, pressure, magnetic field, and so on [3–6]. The laser media are among the most important parts of orthogonally polarized dual-wavelength lasers. Many laser crystals, optically, are biaxial and anisotropic, such as Nd-doped vanadates, Nd:YLiF<sub>4</sub>, Nd:KG(WO<sub>4</sub>)<sub>2</sub>, and Nd:YAP. Anisotropic laser crystals have many remarkable advantages

over isotropic ones. The gain coefficient, polarization, and wavelength of stimulated emission can be varied with the crystallographic orientation of anisotropic laser crystals, which provides the capability for optimizing particular performance characteristics. Among the various Nd-doped crystals, Nd:YAP crystal is an important candidate for orthogonally polarized dual-wavelength lasers. This is because Nd:YAP crystal not only possesses high thermal conductivity and an excellent optomechanical coefficient but also has a large stimulated emission cross section [7]. Moreover, the large natural birefringence of Nd:YAP may overcome the limitations on fundamental mode operation and depolarization losses caused by thermally induced stress birefringence and bifocusing at high average powers [8]. Recently, Nd:YAP,

Nd:GdVO<sub>4</sub>, and Nd:LuVO<sub>4</sub> lasers based on the  $^4F_{3/2}$ – $^4I_{11/2}$  transition have been demonstrated for achieving dual-wavelength emission with orthogonal polarizations, in which a polarization beam splitter (PBS) [9,10] or an intracavity etalon [11] was employed. Such an orthogonally polarized dual-wavelength laser with a smaller separation would be especially valuable as a compact and strong laser source to generate terahertz emission because the frequency difference [12] between two polarizations is about 0.9 THz. Coherent THz waves, traditionally defined in the frequency range of 0.1–3 THz, have great potential for THz imaging, sensing, and THz spectroscopy applications [13–15]. The diagram of energy levels of Nd<sup>3+</sup> in Nd:YAP crystal is shown in Fig. 1 [16]. The wavelength of the strongest line comes from the  $^4F_{3/2}$ – $^4I_{11/2}$  transition. The  $^4F_{3/2}$ – $^4I_{13/2}$  transition has two intense overlapped stark transitions: R1–X1 at 1339 nm and R2–X3 at 1341 nm. The stimulated emission cross sections vary with polarization in the anisotropic Nd:YAP crystal [17]. In 2012, we reported a diode-pumped cw orthogonally polarized dual-wavelength Nd:YAP laser at 1064.5 and 1079.5 nm with a PBS [9]. In this work, we will present our recent results of exploring a dual-wavelength Nd:YAP laser. By adjusting the tilt angle of an uncoated glass plate inserted in the laser cavity, we can control the cavity losses of two polarized directions. We experimentally accomplish a cw dual-wavelength Nd:YAP laser with orthogonal *a*- and *c*-axis polarizations at 1339 and 1341 nm, respectively. At an incident pump power of 17.3 W, cw output powers of 1.6 W at 1339 nm and of 2.3 W at 1341 nm are simultaneously obtained. Furthermore, intracavity sum-frequency mixing at 1339 and 1341 nm was then realized in a KTP crystal to reach the red range. We obtained a maximum cw output power of 558 mW at 670 nm.

## 2. Experiment and Result Analysis

The experimental setup used is described in Fig. 2(a). The optical pumping was done by using fiber-coupled (diameter of 400 μm and numerical aperture NA = 0.22) diode lasers from Coherent Co., USA. The 803 nm emitting diode produced 20 W of pump

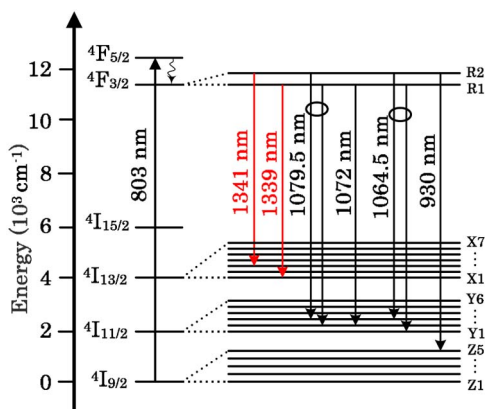


Fig. 1. Energy structure of a Nd:YAP crystal.

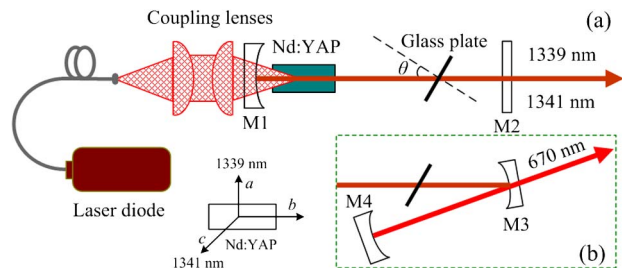


Fig. 2. Experimental setups for (a) orthogonally polarized dual-wavelength Nd:YAP laser at 1341 and 1339 nm and (b) their sum-frequency mixing.

power with an emission bandwidth of 2.5 nm (FWHM definition). The coupling optics consists of two identical plano-convex lenses with focal lengths of 15 mm used to reimage the pump beam into the laser crystal at a ratio of 1:1. The coupling efficiency is 95%. A *b*-axis 1.0 at. % Nd<sup>3+</sup>-doped Nd:YAP crystal with dimensions of 8 mm in length and 3 mm in diameter was used as the laser rod. For our pump beam, the absorption coefficient was measured to  $\alpha = 7.2 \text{ cm}^{-1}$ . This corresponds to an overall absorption of 99.7%. The measurements were done at room temperature. The Nd:YAP crystal was wrapped with indium foil and mounted on a thermoelectric cooled (TEC) copper block, and the temperature was maintained at 20°C. The whole cavity was also cooled by TEC. Both sides of the laser crystal were coated for high transmission (HT) at 1339 and 1341 nm. The input mirror was a 100 cm radius-of-curvature concave mirror with antireflection coating at 803 nm on the entrance face and with high reflectance (HR) coating near 1340 nm and HT coating at 803 nm on the second surface. The output coupler was a flat mirror with transmission of 5.3% near 1340 nm and HT from 1060 to 1080 nm for suppressing the strongest line coming from the  $^4F_{3/2}$ – $^4I_{11/2}$  transition. An uncoated glass plate with a thickness of 0.3 mm was placed in the cavity. The cavity length was approximately 20 mm.

First of all, we investigate the Nd:YAP laser output performance without the glass plate. For  $^4F_{3/2}$ – $^4I_{13/2}$  transition of the *b*-axis laser rod, the gain is greatest for 1341 nm with the polarization of the *c*-axis direction and greatest for 1339 nm with the polarization of the *a*-axis direction. Because the gain of the *c*-axis polarized laser is much greater than that of the *a*-axis polarized laser without polarization-selective optics, the oscillation in the laser cavity is always obtained with the *c*-axis polarized laser. Many experiments have shown that Nd:YAP crystal was an excellent laser material for operation at 1.3 μm [18–20]. Figure 3 presents the dependence of the output power on the incident pump power for the single-wavelength Nd:YAP laser at 1341 nm. The pump threshold is 3.2 W. The maximum output power reaches 5.6 W at 17.3 W of incident pump power. The corresponding optical conversion efficiency is 32.4% with a slope efficiency of approximately 42.2%. The measured optical spectrum at

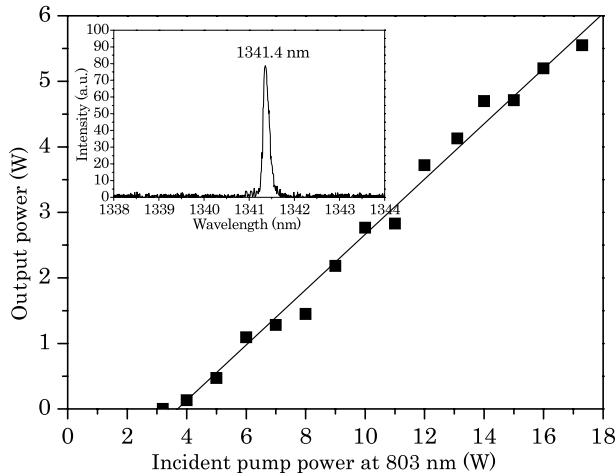


Fig. 3. Output power versus the incident pump power for the 1341 nm emission. Inset: optical spectrum of the 1341 nm emission at the maximum output power.

the maximum output power is depicted in the inset of Fig. 3. The beam quality factor  $M^2$  is 1.12, as measured by the knife-edge technique [21], which shows that the laser output at 1341 nm is operating at the TEM<sub>00</sub> mode. The spectral linewidth (FWHM) is about 0.4 nm with the central wavelength at 1341.4 nm. Note that the present laser output is linearly polarized along the  $c$ -axis direction.

Usually, simultaneous dual-wavelength operation with the same laser medium in the same cavity is rather difficult because of strong gain competition between the two wavelengths. The oscillation condition of the simultaneous multiple-wavelength laser has been derived and used to analyze the possibility of simultaneous dual-wavelength lasers in various neodymium host crystals [22–31]. This research about Nd:YAP 1.3  $\mu$ m lasers just focused on single wavelength. To the best of our knowledge, the study of 1.3  $\mu$ m orthogonally polarized dual-wavelength Nd:YAP lasers has scarcely been reported to date. According to the threshold condition of the diode-end-pumped solid-state four-level laser [32,33], the ratio of laser thresholds  $\gamma$  for two wavelengths of  $c$ -axis polarization and  $a$  axis polarization can be expressed as

$$\gamma = \frac{P_{th,2}}{P_{th,1}} = \frac{\ln(1/R_2) + L_2 \eta_1 f_1 \sigma_1}{\ln(1/R_1) + L_1 \eta_2 f_2 \sigma_2} \frac{1 - \exp(-2\omega_p^2/\omega_1^2)}{1 - \exp(-2\omega_p^2/\omega_2^2)}, \quad (1)$$

where  $R_i$  is the reflectivity of the output mirror,  $L_i$  is the roundtrip cavity excess losses at the corresponding transition wavelength,  $\eta_i$  is the quantum efficiency,  $h\nu_p$  is the pump photon energy,  $\sigma_i$  is the emission cross section,  $\tau$  is the fluorescence lifetime,  $\omega_p$  is the pump beam waist in the active medium,  $\omega_i$  is the laser beam waist, and  $f_i$  is the fractional thermal population in the Stark components of the upper laser levels. The 1339 and 1341 nm emissions

originate from the first and second Stark components ( $R_1$ ,  $R_2$ , namely 11,542 and 11,419  $\text{cm}^{-1}$  [16], fractional thermal population at the room temperatures of  $f_1 = 0.36$  and  $f_2 = 0.64$ ) of the R1 and R2 lines of the  $^4F_{3/2}$  manifold, respectively. Here,  $i = 1$  and 2 represents the two wavelengths of  $a$ - and  $c$ -axis polarization, respectively. Since  $R_1 \approx R_2$ ,  $\sigma_1 < \sigma_2$ ,  $\eta_1 \approx \eta_2$ ,  $f_1 < f_2$ , and  $\omega_1 \approx \omega_2$ , the ratio  $\gamma$  is less than 1 without introducing the deliberate difference for losses  $L_1$  and  $L_2$ . The result of  $\gamma < 1$  indicates that the laser will be dominated at 1341 nm. To obtain orthogonally polarized dual-wavelength operation at 1339 and 1341 nm, an appropriate difference for losses  $L_1$  and  $L_2$  needs to be introduced to reach the condition of  $\gamma \geq 1$ . For achieving the difference for losses  $L_1$  and  $L_2$ , an uncoated glass plate was inserted into the laser cavity. In our experiment, the  $c$  axis of Nd:YAP crystal is set to be placed in the vertical direction, and the angle of inclination of the glass plate is relative to the optical axis of the resonator, where the plane of incidence is in the horizontal direction. As a result, the  $c$ - and  $a$ -axis polarized waves are perpendicular and parallel to the plane of incidence, corresponding to the  $s$  and  $p$  waves, respectively. The inclined angle of the glass plate is equal to the incident angle of light. In terms of incident angle  $\theta$ , the losses caused by the Fresnel reflection [34] for  $s$  and  $p$  waves are given in Fig. 4. It can be seen in Fig. 4 that the overlapping curves for the losses  $L_s$  and  $L_p$  are at the small incident angle, and then gradually separate.

When the incident angle  $\theta$  was adjusted around  $25^\circ$  and the incident pump power was increased to about 5.2 W, the dual-wavelength laser at 1339 and 1341 nm started to oscillate simultaneously. Figure 5 shows results on simultaneous dual-wavelength emission at 1339 and 1341 nm. At an incident pump power of 17.3 W, the output powers of 1.6 W at 1339 nm and of 2.3 W and 1341 nm are simultaneously obtained. A total output power of 3.9 W was achieved with optical conversion efficiency of 22.5%. It can be seen in Fig. 5 that the output powers of both

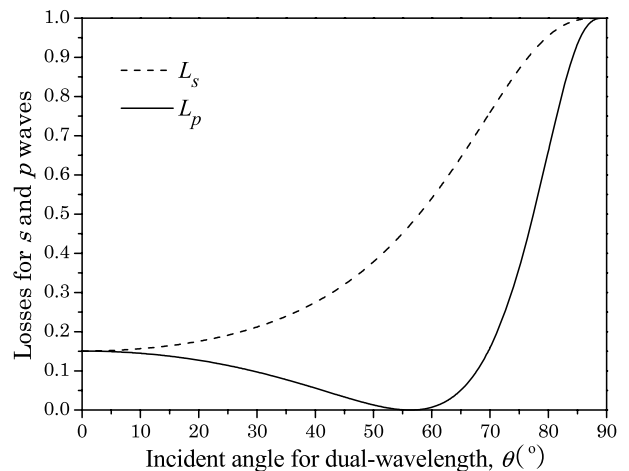


Fig. 4. Dependence of the losses for  $s$  and  $p$  waves on the incident angle for dual-wavelength operation.

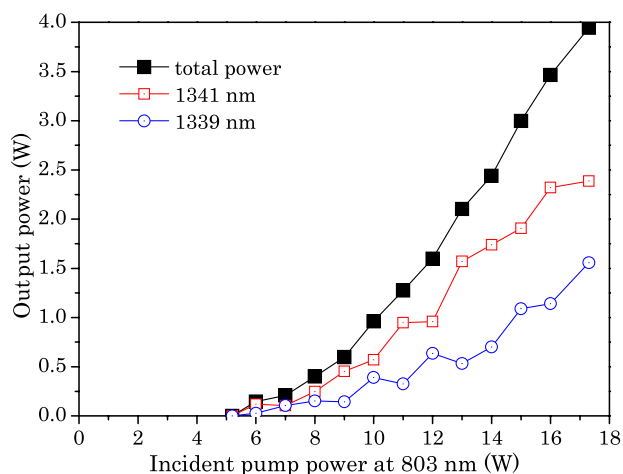


Fig. 5. Dependence of the relative output powers at 1339 and 1341 nm on the incident pump power.

wavelengths linearly increased as the pump power increased. We believe that the competitive interaction between two wavelengths is due to the gain-to-loss balances. The fluctuations for 1339 and 1341 nm lasers at the pump power of 17.3 W are about 4.4% and 3.8%, respectively. The spectrum of the dual-wavelength laser at the pump power of 17.3 W is shown in Fig. 6. The central wavelengths are 1339.2 and 1341.4 nm, with optical spectral line-widths of 0.25 and 0.35 nm, respectively.

When the incident angle  $\theta$  was adjusted around  $35^\circ$ , we found that the laser first emits radiation at the weaker line at 1339 nm. Figure 7 shows results for the dual-wavelength emission at 1339 and 1341 nm. As can be seen from Fig. 7, the threshold of lasing at 1339 nm decreased to 6.2 W and the output power increased monotonically up to 3.0 W for 17.3 W of pump power. The 1341 nm laser emission started to oscillate at an increased threshold of 4.1 W and reached a maximum output power of 1.6 at 13.2 W of pump power, with a strong decrease beyond this pump power. We believe that the gain competition between 1341 and 1339 nm lines leads to the output power of 1341 nm decreasing over 13.2 W of pump power.

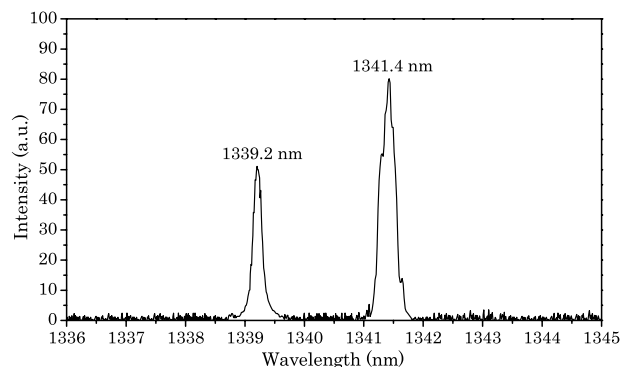


Fig. 6. Optical spectrum of dual-wavelength operation at the maximum output power.

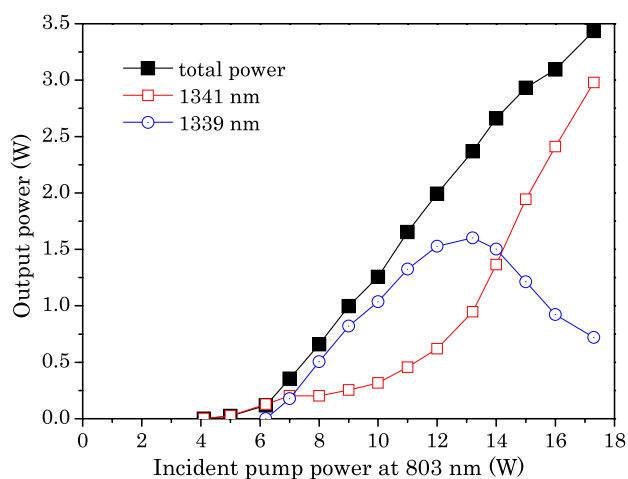


Fig. 7. Dependence of the relative dual-wavelength output powers at 1339 and 1341 nm on the incident pump power.

As the best performance was obtained for the orthogonally polarized dual-wavelength Nd:YAP laser, we tried second-harmonic generation (SHG) at  $1.3 \mu\text{m}$ . The cw intracavity frequency doubling of a laser diode-pumped Nd:YAP laser operating in the  $1.3 \mu\text{m}$  region has been reported [35]. To the best of our knowledge, no research regarding intracavity sum-frequency mixing of  $1.3 \mu\text{m}$  orthogonally polarized dual-wavelength Nd:YAP lasers has been reported to date. To realize efficient sum-frequency mixing, a V-folded cavity was designed, as shown in Fig. 2(b). The optical pumping, the coupling optics, the input mirror, and the laser crystal were the same as the corresponding ones in the setup of the dual-wavelength laser at 1341 and 1339 nm mentioned above. The concave mirror M3 ( $\text{Roc} = -50 \text{ mm}$ ) is an output coupler, which was HR coated near 1340 nm, HT coated at 670 nm, and HT coated from 1060 to 1080 nm. The concave mirror M4 ( $\text{Roc} = -200 \text{ mm}$ ) was HR coated at  $1.3 \mu\text{m}$  and 670 nm. A KTP crystal cut for type-II critical phase matching in the principal plane XZ ( $\theta = 58.9^\circ$ ,  $\varphi = 0^\circ$  with  $d_{\text{eff}} = 2.84 \text{ pm/V}$ ) was chosen as the nonlinear crystal. The size of the KTP crystal is  $2 \text{ mm} \times 2 \text{ mm} \times 5 \text{ mm}$ , and both end facets of the KTP crystal are HT coated at  $1.3 \mu\text{m}$  and 670 nm to reduce the reflection losses in the cavity.

At the incident pump power of 17.3 W, we adjusted the tilt angle of the glass plate; the experimental red output power and the pump laser thresholds as a function of the incident angle  $\theta$  are obtained as shown in Fig. 8. As can be seen from Fig. 8, the red laser emission started oscillating at an incident angle of  $10^\circ$  and reached a maximum output power of 558 mW at  $30^\circ$  of incident angle with an optical conversion efficiency of 3.2%, with a strong decrease beyond this incident angle. We believe that the strong loss of the 1341.4 nm line and the gain competition between 1341 and 1339 nm lines leads to the output power of 670 nm decreasing beyond  $30^\circ$  of incident angle. With the incident angle  $\theta$  increasing to around



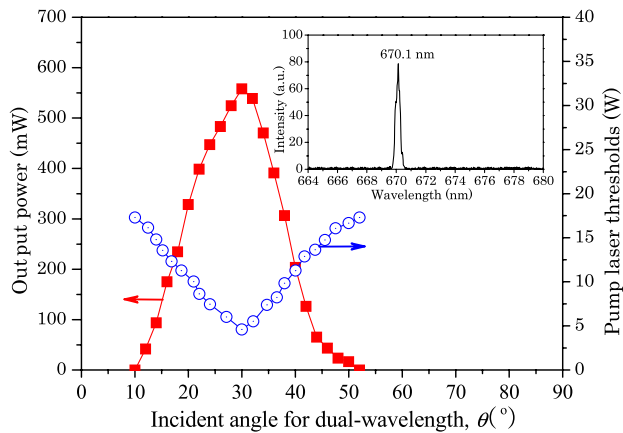


Fig. 8. Dependence of the relative output powers at 670 nm at the maximum pump power and the pump laser thresholds on the tilt angle  $\theta$  of the glass plate.

52°, the gain at 1339.2 nm exceeded far beyond that at 1341.4 nm, and then the former will oscillate instead of the latter. Thus, the red laser at 670 nm cannot be obtained by sum-frequency mixing of both orthogonally polarized lasers. At an output power of 558 mW, the  $M^2$  factors are 1.12 and 1.23 in the  $x$  and  $y$  directions, respectively. The asymmetry of the  $M^2$  factor in two directions is the result of the walk-off between the fundamental wave and the second in the direction of the KTP. The fluctuation of the red output power is about 3.5%. The measured optical spectrum at the maximum output power is depicted in the inset of Fig. 8. The spectral linewidth (FWHM) is about 0.25 nm, with the central wavelength at 670.1 nm.

### 3. Conclusion

A diode-pumped cw orthogonally polarized dual-wavelength laser at 1339 and 1341 nm has been experimentally demonstrated. An uncoated glass plate was placed in the laser cavity to control the loss of the strong emission. The output wavelengths are 1339 nm in  $a$ -axis polarization and 1341 nm in  $c$ -axis polarization, respectively, which are orthogonal to each other. At an incident pump power of 17.3 W, the output power obtained at 1339 and 1341 nm is 1.6 and 2.3 W, respectively. After SHG, a cw red laser was also demonstrated through sum-frequency mixing at the two orthogonally polarized wavelengths. The maximum output power of 558 mW at 670 nm was achieved with type-II critical phase-matched KTP crystal. We believe that the method to control cavity loss to realize the simultaneous dual-wavelength laser with orthogonal polarizations in this paper can be extended to other polarization-dependent solid-state lasers, such as those with host materials of vanadates,  $\text{YLiF}_4$ , or  $\text{KG}(\text{WO}_4)_2$  for orthogonally polarized dual-wavelength output.

This work was supported by the National Natural Science Foundation of China (Grant Nos. 61108029 and 61275135).

### References

1. L. G. Fei and S. L. Zhang, "The discovery of nanometer fringes in laser self-mixing interference," *Opt. Commun.* **273**, 226–230 (2007).
2. S. L. Zhang, Y. D. Tan, and Y. Li, "Orthogonally polarized dual frequency lasers and applications in self-sensing metrology," *Meas. Sci. Technol.* **21**, 054016 (2010).
3. S. Zhang and D. Li, "Using beat frequency lasers to measure micro-displacement and gravity: a discussion," *Appl. Opt.* **27**, 20–21 (1988).
4. S. Zhang, M. Wu, and G. Jin, "Birefringent tuning double frequency He-Ne laser," *Appl. Opt.* **29**, 1265–1267 (1990).
5. J. Zhang, T. Feng, S. Zhang, and G. Jin, "Measurements of magnetic fields by a ring laser," *Appl. Opt.* **31**, 6459–6462 (1992).
6. Y. Ding, S. Zhang, Y. Li, J. Zhu, W. Du, and R. Suo, "Displacement sensors based on feedback effect of orthogonally polarized lights of frequency-split HeNe lasers," *Opt. Eng.* **42**, 2225–2228 (2003).
7. H. Y. Shen, T. Q. Lian, R. R. Zeng, Y. P. Zhou, and G. F. Yu, "Measurement of the stimulated emission cross section for the  $^4\text{F}_{3/2}$ - $^4\text{I}_{13/2}$  transition of  $\text{Nd}^{3+}$  in  $\text{YAlO}_3$  crystal," *IEEE J. Quantum Electron.* **25**, 144–146 (1989).
8. G. A. Massey, "Criterion for selection of cw laser host materials to increase available power in the fundamental mode," *Appl. Phys. Lett.* **17**, 213–215 (1970).
9. Y. F. Lü, P. Zhai, J. Xia, X. H. Fu, and S. T. Li, "Simultaneous orthogonal polarized dual-wavelength continuous-wave laser operation at 1079.5 nm and 1064.5 nm in  $\text{Nd}:\text{YAlO}_3$  and their sum-frequency mixing," *J. Opt. Soc. Am. B* **29**, 2352–2356 (2012).
10. B. Wu, P. P. Jiang, D. Z. Yang, T. Chen, J. Kong, and Y. H. Shen, "Compact dual-wavelength  $\text{Nd}:\text{GdVO}_4$  laser working at 1063 and 1065 nm," *Opt. Express* **17**, 6004–6009 (2009).
11. Y. P. Huang, C. Y. Cho, Y. J. Huang, and Y. F. Chen, "Orthogonally polarized dual-wavelength  $\text{Nd}:\text{LuVO}_4$  laser at 1086 nm and 1089 nm," *Opt. Express* **20**, 5644–5651 (2012).
12. W. Shi, Y. J. Ding, N. Fernelius, and K. Vodopyanov, "Efficient, tunable, and coherent 0.18–5.27-THz source based on GaSe crystal," *Opt. Lett.* **27**, 1454–1456 (2002).
13. J. F. Federici, B. Schulkin, F. Huang, D. Gary, R. Barat, F. Oliveira, and D. Zimdars, "THz imaging and sensing for security applications—explosives, weapons and drugs," *Semicond. Sci. Technol.* **20**, S266–S280 (2005).
14. J. B. Baxter and G. W. Guglietta, "Terahertz spectroscopy," *Anal. Chem.* **83**, 4342–4368 (2011).
15. C. B. Reid, E. Pickwell-MacPherson, J. G. Laufer, A. P. Gibson, J. C. Hebden, and V. P. Wallace, "Accuracy and resolution of THz reflection spectroscopy for medical imaging," *Phys. Med. Biol.* **55**, 4825–4838 (2010).
16. M. J. Weber and T. E. Varitimos, "Optical spectra and intensities of  $\text{Nd}^{3+}$  in  $\text{YAlO}_3$ ," *J. Appl. Phys.* **42**, 4996–5005 (1971).
17. G. A. Massey and J. M. Yarborough, "High average power operation and nonlinear optical generation with the  $\text{Nd}:\text{YAlO}_3$  laser," *Appl. Phys. Lett.* **18**, 576–579 (1971).
18. H. Zhu, C. Huang, G. Zhang, Y. Wei, L. Huang, J. Chen, and Z. Chen, "High-power CW diode-side-pumped 1341 nm  $\text{Nd}:\text{YAP}$  laser," *Opt. Commun.* **270**, 296–300 (2007).
19. Y. Wei, G. Zhang, C. H. Huang, H. Y. Zhu, L. X. Huang, X. J. Ou-Yang, and G. F. Wang, "A single wavelength 1339 nm  $\text{Nd}:\text{YAP}$  pulsed laser," *Opt. Commun.* **282**, 4397–4400 (2009).
20. A. Li, H. Zhu, G. Zhang, C. Huang, Y. Wei, L. Huang, and Z. Chen, "Diode side-pumped 1.3414  $\mu\text{m}$   $\text{Nd}:\text{YAP}$  laser in Q-switched mode," *Appl. Opt.* **46**, 8002–8006 (2007).
21. A. E. Siegman, M. W. Sasnett, and T. F. Johnston, "Choice of clip levels for beam width measurements using knife-edge techniques," *IEEE J. Quantum Electron.* **27**, 1098–1104 (1991).
22. B. M. Walsh, "Dual wavelength lasers," *Laser Phys.* **20**, 622–634 (2010).
23. E. Herault, F. Balembois, and P. Georges, "491 nm generation by sum-frequency mixing of diode pumped neodymium lasers," *Opt. Express* **13**, 5653–5661 (2005).

24. N. Pavel, "Simultaneous dual-wavelength emission at 0.90 and 1.06  $\mu\text{m}$  in Nd-doped laser crystals," *Laser Phys.* **20**, 215–221 (2010).
25. H. Y. Shen, R. R. Zeng, Y. P. Zhou, G. F. Yu, C. H. Huang, Z. D. Zeng, W. J. Zhang, and Q. J. Ye, "Simultaneous multiple wavelength laser action in various neodymium host crystals," *IEEE J. Quantum Electron.* **27**, 2315–2318 (1991).
26. Y. F. Chen, "cw dual-wavelength operation of a diode-end-pumped Nd:YVO<sub>4</sub> laser," *Appl. Phys. B* **70**, 475–478 (2000).
27. Y. Lu, B. G. Zhang, E. B. Li, D. G. Xu, R. Zhou, X. Zhao, F. Ji, T. L. Zhang, P. Wang, and J. Q. Yao, "High power simultaneous dual-wavelength emission of an end-pumped Nd:YAG laser using the quasi-three-level and the four-level transition," *Opt. Commun.* **262**, 241–245 (2006).
28. Y. Y. Lin, S. Y. Chen, A. C. Chiang, R. Y. Tu, and Y. C. Huang, "Single-longitudinal-mode, tunable dual wavelength, CW Nd:YVO<sub>4</sub> laser," *Opt. Express* **14**, 5329–5334 (2006).
29. R. Zhou, E. B. Li, B. G. Zhang, X. Ding, Z. Q. Cai, W. Q. Wen, P. Wang, and J. Q. Yao, "Simultaneous dual-wavelength CW operation using  $^4F_{3/2}$ - $^4I_{13/2}$  transitions in Nd:YVO<sub>4</sub> crystal," *Opt. Commun.* **260**, 641–644 (2006).
30. J. L. He, J. Du, J. Sun, S. Liu, Y. X. Fan, H. T. Wang, L. H. Zhang, and Y. Hang, "High efficiency single- and dual-wavelength Nd:GdVO<sub>4</sub> lasers pumped by a fiber-coupled diode," *Appl. Phys. B* **79**, 301–304 (2004).
31. H. Y. Shen, R. R. Zeng, Y. P. Zhou, G. F. Yu, C. H. Huang, Z. D. Zeng, W. J. Zhang, and Q. J. Ye, "Comparison of simultaneous multiple wavelength lasing in various neodymium host crystals at transitions from  $^4F_{3/2}$ - $^4I_{11/2}$  and  $^4F_{3/2}$ - $^4I_{13/2}$ ," *Appl. Phys. Lett.* **56**, 1937–1938 (1990).
32. T. Y. Fan and R. L. Byer, "Diode laser-pumped solid-state lasers," *IEEE J. Quantum Electron.* **24**, 895–912 (1988).
33. K. Lünstedt, N. Pavel, K. Petermann, and G. Huber, "Continuous-wave simultaneous dual-wavelength operation at 912 and 1063 nm in Nd:GdVO<sub>4</sub>," *Appl. Phys. B* **86**, 65–70 (2007).
34. M. Born and E. Wolf, *Principles of Optics: Electromagnetic Theory of Propagation, Interference and Diffraction of Light*, 7th ed. (Cambridge University, 1999).
35. H. Y. Zhu, G. Zhang, C. H. Huang, Y. Wei, L. X. Huang, and Z. Q. Chen, "8.1 W/670.7 nm and 5.1 W/669.6 nm cw red light outputs by intracavity frequency doubling of a Nd:YAP laser with LBO," *Appl. Phys. B* **91**, 433–436 (2008).